Technological University Dublin
ARROW@TU Dublin

Articles

2023

TiO2-MWCNT Nanohybrid: Cytotoxicity, protein corona formation and cellular internalisation in RTG-2 fish cell line

Gabriela Helena Da Silva
Brazilian Nanotechnology National Laboratory, Brazil

Lidiane Silva Franqui
Brazilian Nanotechnology National Laboratory, Brazil

Marcelo A. De Farias
Brazilian Nanotechnology National Laboratory, Brazil

See next page for additional authors

Follow this and additional works at: https://arrow.tudublin.ie/creaart

Part of the Nanotechnology Commons

Recommended Citation

Da Silva, Gabriela Helena; Silva Franqui, Lidiane; De Farias, Marcelo A.; De Castro, Vera Lucia S.S.; Byrne, Hugh; Martinez, Diego S.T.; Monteiro, Regina T.R.; and Casey, Alan, "TiO2-MWCNT Nanohybrid: Cytotoxicity, protein corona formation and cellular internalisation in RTG-2 fish cell line" (2023). *Articles*. 208.
https://arrow.tudublin.ie/creaart/208

This Article is brought to you for free and open access by ARROW@TU Dublin. It has been accepted for inclusion in Articles by an authorized administrator of ARROW@TU Dublin. For more information, please contact arrow.admin@tudublin.ie, aisling.coyne@tudublin.ie, gerard.connolly@tudublin.ie, vera.kilshaw@tudublin.ie.

This work is licensed under a Creative Commons Attribution-Share Alike 4.0 International License.
Funder: Government of Ireland International Education Scholarship (GOI-IES), the National Council for Scientific and Technological Development (CNPq), the Coordenação de Aperfeiçoamento de Pessoal de Nível Superior (CAPES/ Brasil) finance code 001, the National System of Laboratories on Nanotechnologies (SisNANO/MCTIC), the National Institute of Science, Technology and Innovation for Functional Complex Materials (INTC-Inomat) and the São Paulo

Authors
Gabriela Helena Da Silva, Lidiane Silva Franqui, Marcelo A. De Farias, Vera Lucia S.S. De Castro, Hugh Byrne, Diego S.T. Martinez, Regina T.R. Monteiro, and Alan Casey

This article is available at ARROW@TU Dublin: https://arrow.tudublin.ie/creaart/208

1 **TiO_2-MWCNT nanohybrid: Cytotoxicity, protein corona formation and cellular**
2 **internalisation in RTG-2 fish cell line**

3 Gabriela H. Da Silva[1,2,3,4*], Lidiane Silva Franqui[1], Marcelo A. De Farias[1], Vera Lucia S.
4 S. De Castro[3], Hugh J. Byrne[4], Diego S. T. Martinez[1,2], Regina T. R. Monteiro[2], and Alan
5 Casey[4]

6 [1]Brazilian Nanotechnology National Laboratory (LNNano), Brazilian Center for
7 Research in Energy and Materials (CNPEM), Campinas, São Paulo, Brazil

8 [2]Center of Nuclear Energy in Agriculture (CENA), University of São Paulo (USP),
9 Piracicaba, São Paulo, Brazil

10 [3]Laboratory of Ecotoxicology and Biosafety, EMBRAPA Environment, Jaguariúna, São
11 Paulo, Brazil

12 [4]FOCAS Research Institute, TU Dublin, City Campus, Camden Row, Dublin 8, Ireland

13 [*]Corresponding author: gabriela.silva@lnnano.cnpem.br

14

15 **Abstract**

16 Titanium dioxide nanoparticles-multiwalled carbon nanotubes (TiO_2-MWCNT)
17 nanohybrids have enhanced photocatalytic activity across visible light with promising
18 applications in environmental remediation, solar energy devices and antimicrobial
19 technologies. However, little is known about the toxicological properties of TiO_2-
20 MWCNT. In this sense, it is necessary to evaluate the toxicological effects of TiO_2-
21 MWCNT towards the safe and sustainable development of nanohybrids. In this work, we
22 studied the cytotoxicity, protein corona formation and cellular internalisation of TiO_2-
23 MWCNT on fibroblasts derived from gonadal rainbow trout tissue (RTG-2) for the first
24 time. This nanohybrid did not show any toxic effect on RTG-2 cells up to 100 μg mL^{-1}
25 after 24 h of exposure as monitored by alamar blue, neutral red and trypan blue assays (in
26 the presence or absence of fetal bovine serum, FBS). Furthermore, cryo-transmission
27 electron microscopy analysis demonstrated that TiO_2 particles were attached to the
28 surface of nanotubes after FBS-protein corona formation in a cell culture medium. Raman
29 spectroscopy imaging showed that TiO_2-MWCNT could be internalised by RTG-2 cells.
30 This work is a novel contribution towards better understanding the nano-bio interactions
31 of nanohybrids linked to their in vitro effects on fish cells in aquatic nanoecotoxicology.

32 **Keywords:** Nanosafety, Protein corona, Raman, Ecotoxicity.

33

34 ## 1. Introduction

35 Nanohybrid materials have been attracting increasing attention for health, energy
36 and environmental (Belkhanchi et al., 2021, 2020; Sharma et al., 2021; Yoon et al., 2021).
37 Combining two or more nanomaterials (NMs) to form nanohybrids can generate new
38 functionalities and/or enhanced properties (Saleh et al., 2014). In this sense, the
39 combination of titanium dioxide nanoparticles (TiO_2) and multi-walled carbon nanotubes
40 (MWCNT) is particularly interesting in producing a nanohybrid material. TiO_2 is a widely
41 used nanoparticle with low synthesis cost, high photostability and photocatalytic activity
42 (Nasr et al., 2018). Due to its large band gap (3.3 eV), this particle only absorbs in the
43 near UV region. Therefore, there has been an intensive effort to reduce the bandgap of
44 TiO_2 so that it absorbs in visible regions of the spectrum (Hernández-Alonso et al., 2009).
45 MWCNTs have good mechanical stability, electronic properties, and large surface area,
46 acting as electron donor and enhancing the photocatalytic activity of TiO_2 (Olowoyo et
47 al., 2019; Sharma et al., 2021). In this context, the combination of TiO_2 and carbon
48 nanotubes creates a composite with an increased photocatalytic activity, extended to
49 visible light (Da Dalt et al., 2013; Da Silva et al., 2018; Hemalatha et al., 2015; Nasr et
50 al., 2018). Consequently, this nanohybrid shows promising properties, especially for
51 environmental applications, in which it has been demonstrated to be efficient for the
52 degradation of several dyes and pollutants (Chen et al., 2011; Da Silva et al., 2018; Hamid
53 et al., 2014; Zhao et al., 2010; Zouzelka et al., 2016). Besides, it can also be applied for
54 energy storage (Guler et al., 2015; Mombeshora et al., 2022), photovoltaic energy
55 conversion (Muduli et al., 2009; Wang et al., 2015), renewable energy (Lee et al., 2007;
56 Muduli et al., 2009), sensors (Chen et al., 2022; Sánchez et al., 2007), bactericidal activity
57 (W. Oh et al., 2009), among others.

58 Although nanohybrid production and technology can bring many benefits, as the
59 particles present new and enhanced properties, the impact on the environment or human
60 health may differ from that of the constituent components. Therefore, the safe-by-design
61 approach, including a minimum amount of information about the material's physical-
62 chemical properties, such as size distribution, morphology and surface charge, colloidal
63 behaviour, like aggregation and sedimentation, and toxicity assessment, are crucial
64 towards a safe application and commercialisation of these materials. This approach steps

65 forward to a sustainable and responsible nanotechnology innovation, preventing
66 hazardous impacts on human and environmental health (de Medeiros et al., 2021).

67 TiO_2-MWCNT synthesis, characterisation, and toxicity evaluation towards
68 zebrafish embryos have previously been reported by our research group (Da Silva et al.,
69 2018). This nanohybrid was synthesised with an easy and eco-friendly technique and
70 proved safe for zebrafish embryo development. However, micro-X-ray fluorescence
71 indicated the ingestion of the material by embryos, which may cause effects at the cellular
72 level. Fundamentally, all toxicological responses are related to an impairment of some
73 aspect of cellular activity, for example, cellular uptake, effects on cell signalling,
74 membrane perturbations, production of cytokines, chemokines, ROS, cell necrosis or
75 apoptosis, among others. Those responses often reflect on some physiologic responses
76 observed during *in vivo* testing. Hence, in some cases, *in vitro* assays present a reasonable
77 correlation with *in vivo* (Bols et al., 2005; Di Ianni et al., 2021; Jones and Grainger, 2009;
78 Scott et al., 2021). Another advantage is that *in vitro* tests allow an extensive screening
79 of effects using a small amount of material. Besides, it can be used as an alternative for
80 *in vivo*, relying on the principle of the "3R" aiming to Reduce, Refine and Replace animal
81 experiments (Forest, 2022; Quevedo et al., 2021).

82 Fibroblasts derived from gonadal rainbow trout tissue (RTG-2) is a fish cell line
83 commonly used in aquatic toxicity evaluations. The *in vitro* test with this cell line can be
84 proposed as an alternative method for risk assessment studies, being proven to have a
85 reasonable correlation with *in vivo* fish testing (Castaño et al., 1996; Kolarova et al.,
86 2021). A wide range of cytotoxicity standard tests can be performed with this cell line,
87 such as tetrazolium salt reduction (MTT), alamar blue (AB) and neutral red (NR) assays
88 (Fent, 2001; Hernández-Moreno et al., 2022), allowing a fast obtention of a considerable
89 amount of data, ranging from cell metabolic activity, cell membrane integrity,
90 mitochondria toxicity, lysosome toxicity, etc. Thus, this cell line is being extensively used
91 to understand the toxic mechanisms of environmental contaminants. The obtained results
92 can be used to determine the toxicological profile of chemical modes of toxic action, such
93 as oxidative damage, genotoxicity, membrane disruption, and apoptosis, among others.
94 Therefore, the RTG-2 cell line has been extensively used for nanotoxicity studies
95 (Bermejo-Nogales et al., 2017; Casado et al., 2013; Goswami et al., 2022; Klingelfus et
96 al., 2019; Munari et al., 2014; Vevers and Jha, 2008).

97 It is a consensus that the behaviour of NMs in a biological environment (e.g.,
98 colloidal stability, aggregation, sedimentation, adsorption of biomolecules, surface
99 charge) plays a crucial role in nanotoxicology (da Cruz Schneid et al., 2022; Nel et al.,
100 2009; Petry et al., 2019). When in a biological environment, NMs interact with the
101 biomolecules forming a coating on its surface, commonly referred to as a protein corona
102 (when the biomolecules adsorbed are mainly proteins) or biomolecular corona (Monopoli
103 et al., 2012; Paula et al., 2014). Environmental dimensions of protein coronas have been
104 recently considered, showing critical implications for nanoecotoxicology (Wheeler et al.,
105 2021). In fact, the corona formation confers a new biological and ecological identity to
106 nanomaterials that strongly impact their interactions with living organisms and the
107 environment, critically influencing nanomaterial uptake, biodistribution and toxicity
108 (Martinez et al., 2020; Martins et al., 2022; Morozesk et al., 2018; Natarajan et al., 2021).
109 The corona formation can occur not only in the environment but also under controlled
110 experimental conditions, where the presence of biomolecules, such as fetal bovine serum
111 proteins (FBS) present in the cell culture medium, can modulate the toxicological
112 response. Therefore, it is imperative to study the interaction of nanomaterial-corona to
113 understand the toxicological results obtained in nanotoxicological studies. To the best of
114 our knowledge, there are no reports in the literature considering the protein corona
115 formation on TiO_2-MWCNT linked to its toxicity in RTG-2 fish cells.

116 In this work, we studied the cytotoxicity and cellular internalisation of TiO_2-
117 MWCNT nanohybrid on RTG-2 cells, considering the influence of protein corona
118 formation. We have applied an integrated approach using advanced microscopy
119 techniques such as cryogenic transmission electron microscopy, enhanced dark-field
120 hyperspectral microscopy and Raman microspectroscopy to better understand nano-bio
121 interactions, such as protein corona and nanomaterial-cell interactions. Also, we applied
122 an *in vitro* toxicity assessment towards alternative methods in aquatic toxicology and
123 nanosafety research.

124

125 ## 2. Materials and methods

126 ### 2.1. TiO_2-MWCNT nanohybrid material

127 The TiO_2-MWCNT sample used in the present study was previously synthesised
128 and characterised, as reported by Da Silva et al. (2018). Briefly, this sample was prepared

129 by mechanical milling methods from a proportion of 10:3 of TiO_2 (P25 – Degussa Evonik,
130 Essen, Germany) and MWCNT (CNT Co. Ltd). Prior to the experiments, the TiO_2-
131 MWCNT stock dispersion (0.5 mg mL^{-1}) was prepared in ultrapure water by sonication
132 for 1 h in an ultrasonic bath (Cole-Parmer, model 08895-43, USA) and then stored,
133 protected from light, at room temperature until further use.

134

135 **2.2. Dispersion stability and Cryo-TEM analysis**

136 Colloidal stability studies of TiO_2-MWCNT at a concentration of 100 μg mL^{-1} in
137 DMEM, with and without the addition of 10% FBS, were performed with a
138 spectrophotometer (Multiskan GO, Thermo Scientific, UK) by measuring the optical
139 density at 350 nm after 0, 1, 4 and 8 and 24 hours. A Zetasizer Nano ZS90 instrument
140 (Malvern Instruments, UK) was used to evaluate the hydrodynamic diameter (HD) and
141 polydispersity index (PDI) through dynamic light scattering (DLS) and Zeta potential
142 (ZP) by electrophoretic light scattering (ELS). For DLS measurements, all samples were
143 measured using the "General purpose" analysis method at a scattering angle of 173°
144 (backscatter) and the default size analysis parameters as well as a refractive index of 1.59
145 for the polystyrene particle matrix as sample parameter. The obtained results were the
146 intensity-weighted harmonic mean particle diameter (Z-Average) and the polydispersity
147 index (PI). For electrophoretic mobility measurements from which zeta potential is
148 deduced, the approximation of Smoluchowski was carried out at a temperature of
149 measurement of 25.0 °C by ELS, voltage selection and attenuation selection were set in
150 the automatic mode, except for stability studies with FBS where the voltage was set for
151 10 V. All analyses were performed in triplicate.

152 Cryo-transmission electron microscopy (Cryo-TEM) was used to determine the
153 synthesis efficiency and evaluate whether the combination of TiO_2 and MWCNT
154 remained intact in the cell culture medium (Dulbecco's modified nutrient medium -
155 DMEM). More traditional TEM preparation techniques demand drying or plastic
156 embedding of the sample. Hence, the sample sometimes corresponds to a distorted
157 version of the original. Cryo-TEM sample preparation is by freezing, this way, images
158 can be generated in a real state of hydration of the sample, which is essentially how it
159 exists in solution, avoiding sample deformation by the microscope vacuum and drying
160 effect. Samples containing 100 μg mL^{-1} of TiO_2-MWCNT in ultrapure water and DMEM,

161 with and without 10% fetal bovine serum (FBS) supplementation, were prepared using a
162 Vitrobot Mark IV specimen preparation unit (Thermo Fischer Scientific, USP). The
163 analysis was performed using the transmission electron microscope (TEM) TALOS
164 F200C (Thermo Fischer Scientific, USA) operating at 200 kV. The images were acquired
165 using a Ceta 16M CMOS camera with 4k by 4k pixels (Thermo Fisher Scientific, USA).
166 The hole grid was analysed for all samples, and two individual analyses were performed.
167 The sample was assessed visually, and no statistical analyses were performed.

168

169 **2.3. Protein corona characterisation**

170 The interaction between the FBS proteins and TiO_2-MWCNT was evaluated by
171 SDS-PAGE gel analysis. Protein corona formation is a highly dynamic process, and its
172 composition may change over time. However, studies have shown that protein corona and
173 their composition are established rapidly (Tenzer et al., 2013). Most studies have revealed
174 that hard corona remains stable after 1 hour of incubation (Docter et al., 2014; Franqui et
175 al., 2019; Lesniak et al., 2012; Lundqvist et al., 2011; Martins et al., 2022). However, to
176 show that for TiO_2-MWCNT 1 hour of incubation was enough to achieve the equilibrium
177 of protein adsorption, we performed the protein incubations with 1 and 24 hours. Briefly,
178 the protein corona was prepared by incubating 100 μg mL^{-1} of TiO_2, MWCNT and TiO_2-
179 MWCNT in DMEM supplemented with 10% of FBS for 1 and 24 hours at 22°C. The
180 temperature was chosen because all cytotoxicity assays were performed at 22°C. After
181 incubation, the dispersion was centrifuged at 20817 g for 1 h at 4°C, followed by three
182 washes with PBS (centrifuging for 30 min at 4°C and 20817 g, discarding the supernatant)
183 for removal of poorly bound and unbound proteins. The pellet obtained, formed by the
184 nanomaterial and strongly bound proteins (hard corona), was resuspended in 100 μL of
185 deionised water and sonicated for 2 min. To extract the proteins, 40 μl of sample buffer
186 and 10 μl of dithiothreitol (DTT) 1:10 were added, followed by another sonication step
187 (2 min), after which the samples were incubated at 99 °C for 3 min. Finally, 15 μl of the
188 sample was loaded onto 15% SDS-PAGE gel (Franqui et al., 2019).

189

190 **2.4. RTG-2 cell line culture conditions**

191 Cell lines derived from fish are widely used for the cytotoxic analysis of
192 environmental contaminants (Galbis-Martínez et al., 2018; Lungu-Mitea et al., 2018;

193 Yurdakök-Dikmen et al., 2018) and nanoparticles (Casado et al., 2013; Morozesk et al., 194 2020; Naha et al., 2009; Naha and Byrne, 2013). Hence, Rainbow trout gonadal tissue 195 cell line (RTG-2) lineage was used for *in vitro* evaluation of TiO_2-MWCNT cytotoxicity 196 assay. This cell line was provided by the Dublin Institute of Technology, FOCAS 197 Research Institute, Ireland. Cells were maintained in DMEM (high glucose and pyruvate; 198 ThermoFisher, USA) supplemented with 10% FBS (sterile, heat-inactivated and free from 199 mycoplasma, Cultilab, Brazil), 100 IU mL^{-1} penicillin, 100 μg mL^{-1} streptomycin, and 25 200 mM 4-(2-hydroxyethyl)-1-piperazineethanesulfonic acid (HEPES). Cultures were 201 maintained in an incubator at 22 ± 1 °C under a normal atmosphere and sub-cultured upon 202 reaching 80% confluence.

203

204 **2.5. Cellular viability assays**

205 Most colorimetric cell viability assays, which verify cell viability by assessing plasma 206 and lysosomal membrane integrity, such as the trypan blue and neutral red assays, 207 respectively, or assess the metabolic activity of cells, such as MTT and alamar blue, can 208 interact with NPs (Breznan et al., 2015; Casey et al., 2007), culminating in false results. 209 Therefore, the use of more than one type of cytotoxicity assay is recommended. For this 210 reason, three standard viability tests, alamar blue, neutral red and trypan blue, were 211 employed to increase data reliability. Besides a NM adsorption, with alamar blue and 212 neutral red without the cells was performed to analyse if nanomaterials were interfering 213 with the cytotoxicity assay. Results are shown in the supplementary material.

214

215 **2.5.1. Alamar blue**

216 Cell viability was analysed by the alamar blue (AB) assay, which has been 217 extensively used as an indicator of the cytotoxicity of nanomaterials. AB fluorometric 218 assay is based on the nonspecific, enzymatic, irreversible reduction of the resazurin 219 compound to resorufin by viable cells (MITJANS, 2018). Briefly, 96-well cell culture 220 plates (Flat Bottom, TC Treated, sterile – NEST) were seeded with a cell density of $2x10^5$ 221 cells per mL and allowed to attach overnight. Subsequently, serial dilutions of TiO_2- 222 MWCNT in DMEM (concentration ranging from 0.078 to 100 mg L^{-1}), with and without 223 the addition of 10% FBS, were added and the plates were incubated for 24 hours, at 22 ± 224 1 °C under normal atmosphere. After the exposure, cells were washed with sterile 225 phosphate buffered saline (PBS) and incubated for 3 hours at 22°C with 100 μL of DMEM

226 containing 10% of alamar blue reagent. Fluorescence was measured using an excitation
227 wavelength of 530 nm and an emission wavelength of 595 nm on a multi-plate reader
228 (Spectra Max—M3).

229 **2.5.2. Neutral red**

230 Neutral Red (NR) is an indicator of cell survival based on the ability of viable
231 cells to incorporate and retain NR dye in the lysosomes. Toxic substances cause a
232 decrease in NR uptake, such that spectrophotometric measurements indicate cell viability
233 (BOLS et al., 2005). The exposure was done similarly to alamar blue. After exposure,
234 cells were washed with PBS and incubated for 3 hours at 22 °C with 100 µL of DMEM
235 containing 1.25 µL of NR stock (4 mg mL^{-1}). After incubation, cells were washed with
236 PBS, and 150 µl of the reaction solution (1% acetic acid, 50% ethanol and 49% distilled
237 water) was added. The plate was shaken for 10 min at 240 rpm, and then the absorbance
238 at 540 nm was recorded (Multiskan GO, Thermo Scientific, UK).

239 **2.5.3. Trypan blue**

240 Colorimetric assays can often lead to false results in NM cytotoxicity assays
241 (CASEY et al, 2007). Thus, trypan blue viability assay was used as an alternative to
242 colorimetric assay. The principle of this assay is that living cells with intact cell
243 membranes exclude the trypan blue stain, whereas dead cells do not. Hence, the trypan
244 blue assay consists of a simple assay to determine the number of viable cells in a cell
245 suspension (Stone, Johnston, & Schins, 2009). $2x10^5$ cells per mL were platted in a 96-
246 well plate and allowed to attach overnight. Cells were then exposed to 1, 10 and 100 mg
247 L^{-1} of TiO_2-MWCNT in DMEM (with and without 10% FBS) for 24h at 22 °C.
248 Subsequently, cells were washed with PBS, and 30 µL of trypsin was added to each well,
249 after 5 minutes 100 µL of DMEM were added, and the suspension was centrifuged for 1
250 min at 1500 rpm. The pellet was resuspended in 10 µL of DMEM and 10 µL of trypan
251 blue reagent. Cells were counted in a Neubauer chamber, and cell numbers were
252 calculated.

253 **2.6. Cell cycle**

254 Cell cycle studies were performed to determine whether there were any
255 differences between the cyclic behaviour of the cells. Briefly, to monitor the cell cycle,
256 cells were seeded in T-25 cm^2 flasks at a density of 2×10^6 cell per mL (5 mL of DMEM)
257 and allowed to attach overnight. Subsequently, cells were exposed for 24 hours (in at

258 normal atmosphere and 22 °C) to 1 mg L^{-1} of TiO_2-MWCNT (higher concentrations
259 caused clumping of cells, interfering with the analysis). After exposure, the cells were
260 washed with PBS three times and harvested by enzymatic removal (trypsin). They were
261 fixed in 70% ethanol for 30 minutes, centrifuged (1400 rpm) for 5 minutes and washed
262 with PBS twice. Next, cells were treated with 100 µg mL^{-1} of ribonuclease for 5 min,
263 stained with 50 µg mL^{-1} propidium iodide and incubated for 20 min, after which they
264 were immediately analysed. A minimum of 10,000 single-cell events per sample were
265 analysed with a BD AccuriTM C6 Flow Cytometer.

266

267 **2.7. Enhanced dark-field hyperspectral microscopy**

268 RTG-2 cells were seeded on common microscopy coverslips at a density of $1x10^5$
269 cells per coverslip in 3 mL of DMEM supplemented with 10% FBS and allowed to attach
270 overnight. The coverslips were placed in a 6-well plate and pre-treated with a 1% gelatine
271 solution to increase cell adhesion. After this period, cells were exposed for 24 hours to 1
272 mg L^{-1} of TiO_2-MWCNT in DMEM, with and without FBS supplementation (10%).
273 Subsequently, cells were washed three times with PBS and fixed with glutaraldehyde
274 (2%). For the analysis, cells were kept in ultrapure water. An Olympus microscope (BX-
275 53, Japan) coupled with a VNIR hyperspectral camera (Cytoviva, Inc., Alabama) and a
276 high-resolution dark field capacitor (numerical aperture; NA 1.2-1.4) were used. This
277 system provides a resolution of 90 nm, with excellent contrast and signal-to-noise ratio.
278 Samples were analysed using a 100x immersion objective (Olympus UPlanFLN 100x,
279 1.3 NA). Conventional dark-field images were collected with a Dagexcel-M camera
280 (Dage-MTI, Michigan, IN). The spectral images were analysed using ENVI 4.8 software.
281 The software tool "filter particle" was used to avoid false positives, which removed all
282 control spectra from the treatment. In this way, the spectra present in the map
283 corresponded only to the NM spectra.

284

285 **2.8. Raman microspectroscopy**

286 To evaluate whether the TiO_2-MWCNT had the potential of cellular
287 internalisation, Raman microspectroscopy was used. For this analysis, RTG-2 cells were
288 seeded on calcium fluoride (CaF_2) discs at a density of $2x10^5$ cells per disc with 3 mL of
289 DMEM supplemented with 10% FBS and allowed to attach overnight. Subsequently, they

290 were exposed for 24 hours to 1 mg L^{-1} of TiO_2-MWCNT in DMEM, with and without
291 supplementation of FBS (10%). Afterwards, the medium was removed, cells were washed
292 three times with PBS, fixed with formalin for 3 min and kept in ultrapure water until the
293 analysis. A Horiba Jobin-Yvon LabRAM HR800 spectrometer, equipped with a diode
294 laser with an excitation line at 532 nm, power of 50mW and a 100x immersion objective
295 (LUMPlanF1, Olympus, NA 1.00), was used. The spectrum, from 300 cm^{-1} to 3200 cm^{-}
296 ^{1}, was obtained with a grating of 600 lines/mm and a confocal aperture of 100 µm. The Z
297 axis (depth) map was acquired from the cytoplasmic region of 3 different cells for each
298 treatment, with 20 points and 0.5 µm increment, in the Z direction. The acquisition time
299 was 20 seconds.

300

301 **2.9. Statistical analysis**

302 All tests were performed in triplicates and with three individual repetitions, the
303 statistical analysis was carried out using OriginPro 2022 software (OriginLab). All data
304 were tested for normality using the Kolmogorov_Smirnov test and for homogeneity of
305 variance by Brown-Forsythe test. If parameter assumptions of normal distribution and
306 homogeneity of variance were met, ANOVA was followed by Dunnet's test to compare
307 the data. Where the assumptions were not met, data were analysed using the
308 nonparametric Kruskas-Wallis ANOVA followed by Dunn’s test of multiple
309 comparisons.

310

311 **3. Results and discussion**

312 Accurate characterisation of the NM state in the biological medium is essential to
313 determine their potential adverse effects. The colloidal stability of the TiO_2-MWCNT
314 dispersion in Dulbecco's Modified Eagle's Medium (DMEM), with and without the
315 addition of fetal bovine serum (FBS) (10%), was evaluated by ultraviolet-visible
316 spectroscopy (UV-vis) (Figure 1), indicating the loss of absorbance as a function of time
317 due to sedimentation. Hydrodynamic diameter, polydispersity index (PDI) and zeta
318 potential were analysed by dynamic light scattering (DLS) and electrophoretic light
319 scattering (ELS) measurements (Zetasizer, Malvern Instrument) (Table 1). In ultrapure
320 water and DMEM, TiO_2-MWCNT was highly unstable, resulting in agglomeration and
321 sedimentation (Figure 1). Since oxygenated groups are responsible for promoting the

322 colloidal stability of oxidised multiwalled carbon nanotubes (ox-MWCNT), the low
323 stability of this nanomaterial may be a consequence of TiO_2 binding to these groups.
324 Besides, the media salts facilitate counter ion migration into the solvation layer of
325 nanoparticles decreasing electrostatic forces, also a elevate ionic strength in media can
326 increase Van der Waals force of attraction between particles, this increases aggregation
327 and sedimentation of particles (Das et al., 2022; Parsai and Kumar, 2019). Similar
328 behaviour was observed by Das et al. (2018) when studying the stability of TiO_2-
329 MWCNT. In their studies, it was concluded that the degree of aggregation increased
330 according to increased amounts of TiO_2 in the sample and, consequently, a smaller
331 amount of oxygenated groups available in the MWCNT structure. For TiO_2 nanoparticles,
332 aggregation and sedimentation were also observed when particles were dispersed in
333 DMEM. However, in the presence of proteins, a decrease in both parameters was
334 observed. The same was also observed for carbon nanotubes (CNTs), as several studies
335 have already shown that serum proteins are adsorbed by CNTs, promoting steric
336 stabilisation of the dispersion, reducing the rate of aggregation in biological media (Du et
337 al., 2014; Sacchetti et al., 2013; Wang et al., 2010). In our study, TiO_2-MWCNT exhibited
338 a smaller hydrodynamic size in DMEM with FBS. Hence, FBS proteins cause a decrease
339 in aggregation. However, comparing DLS and UV-Vis data, it is possible to infer that the
340 presence of FBS did not prevent sedimentation but only inhibited aggregation. The same
341 was observed by Allegri et al. (2016) when studying the stability of ox-MWCNT in a
342 protein-rich medium, they observed that, even though ox-MWCNT adsorb a large amount
343 of proteins, they still precipitated over time, consistent with our studies.

344

345

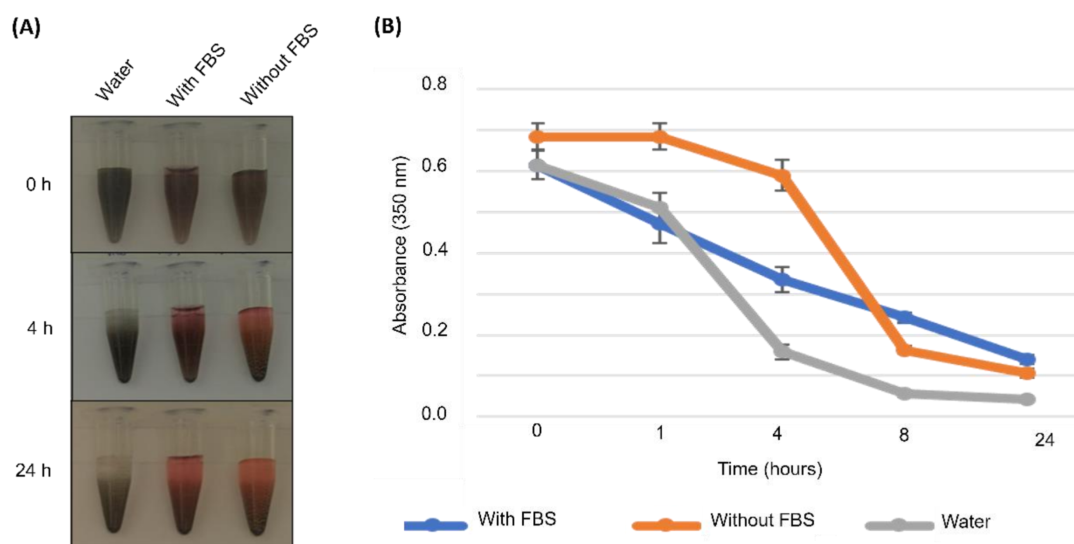

346 **Figure 1.** Stability of TiO_2-MWCNT hybrid nanomaterial in DMEM (with and without
347 the addition of FBS) and ultrapure water for 24 hours. (A) TiO_2-MWCNT Dispersion
348 photograph after 0, 4 and 24h in static conditions (water, media without FBS and media
349 with FBS) and (B) UV-Vis absorbance, of the TiO_2-MWCNT, at 350 nm after 0, 1, 4, 8
350 and 24 hours in static conditions (water, media without FBS and media with FBS).

351

352 **Table 1.** Polydispersity index (PdI) and zeta potential (ZP) of TiO_2-MWCNT suspensions
353 in ultrapure water, DMEM with and without FSB, hydrodynamic diameter (± standard
354 deviation) obtained using DLS and ELS.

Medium	Hydrodynamic diameter (d.nm)	PdI	ZP (mV)
Ultrapure water	741.9 ± 91.6	0.632 ± 0.015	-4.2 ± 0.1
DMEM without FBS	2274.0 ± 337.5	0.683 ±0.185	-12.9 ± 0.7
DMEM with FBS	564.8 ± 51.2	0.646 ± 0.514	-9.0 ± 0.3

355

356 To analyse whether DMEM and/or FBS proteins can modify the morphological
357 characteristics of TiO_2-MWCNT, Cryo-TEM was applied. This technique allowed the *in*
358 *situ* observation of TiO_2-MWCNT in DMEM (with and without FBS supplementation).
359 Our results showed that in all conditions, it was possible to observe tangles of TiO_2-
360 MWCNT, corroborating with the stability results, showing the aggregated state of the
361 materials. Also, it is important to notice that TiO_2 remain bound/attached to TiO_2-
362 MWCNT complex surface in all media conditions, and no free TiO_2 was observed
363 through the Cryo-TEM analysis (Figure 2). These results showed that mechanically
364 milling TiO_2 and MWCNT generate a stable hybrid nanomaterial, as the TiO_2 is strongly

365 bound to MWCNT surface. Besides is important to highlight the applicability of the Cryo-
366 TEM to study nanoparticles organisation and structure in biological media in
367 nanobiotechnology and nanotoxicity evaluations.

368

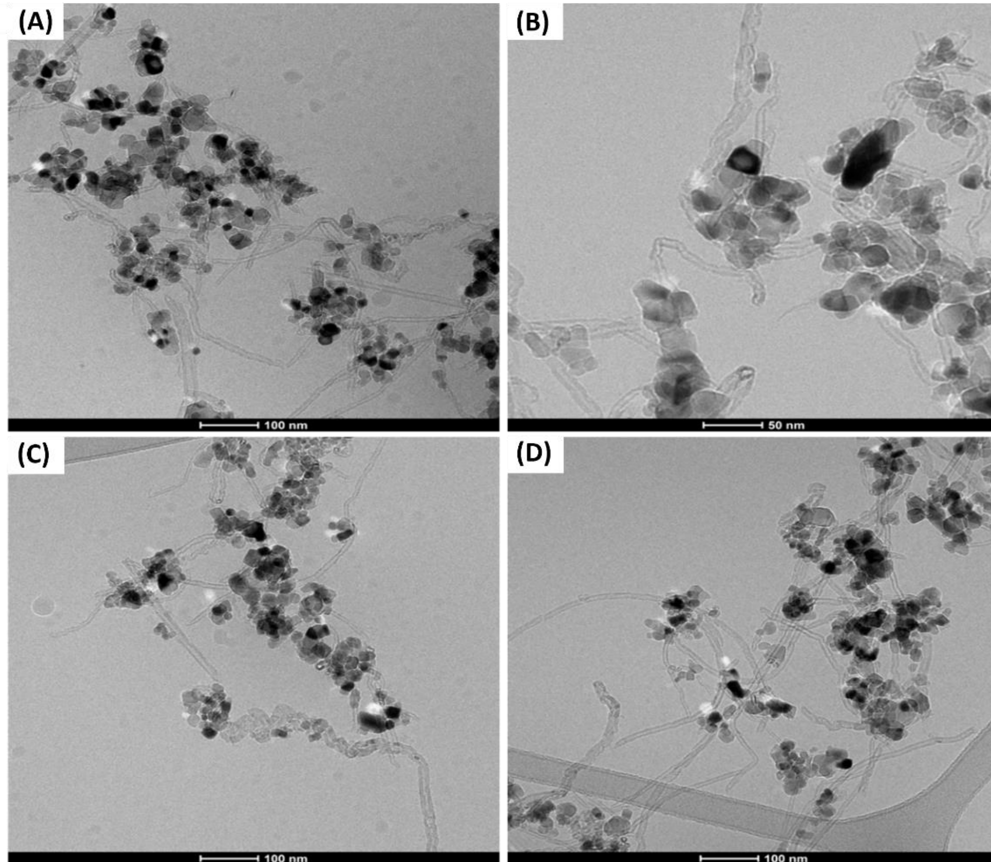

369

370 **Figure 2.** Cryogenic transmission electron microscopy (Cryo-TEM) images of TiO_2-
371 MWCNT (100 mg L^{-1}) in DMEM with FBS (A and B), without FBS (C) and ultra-pure
372 water (D).

373

374 The effect that protein corona coating has on TiO_2 and MWCNT properties and
375 cytotoxicity has already been studied by different authors (Allegri et al., 2016;
376 Borgognoni et al., 2015; Garvas et al., 2015; Long et al., 2018a; Runa et al., 2017; Sit et
377 al., 2019). For example, FBS proteins bound to titanium dioxide nanotubes (TiO_2-NTs)
378 stabilise the dispersion but scavenge photogenerated radicals, preventing the phototoxic
379 effect of UV irradiated TiO_2-NTs, and at low concentrations (1 and 5 µg mL^{-1}) even
380 increasing cell viability for the protein corona coated TiO_2-NTs, as observed by Garvas
381 et al. (2015). Long et al. (2018a) observed that protein corona interaction with pristine
382 and carboxylated MWCNTs causes a change in the diameter and zeta potential of those

383 materials. In their studies, they also observed that the interaction with bovine serum
384 albumin (BSA) increased the internalisation and reduced cytotoxicity of MWCNTs. To
385 our knowledge, our study is the first study addressing the cytotoxicity of TiO_2-MWCNT
386 considering protein corona formation.

387 To understand the interaction between proteins and the TiO_2-MWCNT, TiO_2 and
388 MWCNT were individually used as control samples. Our results showed that 1 hour of
389 incubation is sufficient to achieve the adsorptions equilibrium (Figure 3). TiO_2-MWCNT
390 and MWCNT protein corona were similar; for both, well-defined bands can be seen
391 between 245 and 58 kDa, and at 32, 25 and 11 kDa. However, for TiO_2 NP, only a few
392 well-defined bands between 245 and 58 kDa, and 11 kDa can be observed, indicating a
393 low variety of proteins were adsorbed by this material. TiO_2-MWCNT bound a lower
394 amount of proteins than MWCNT, but a larger variety than TiO_2. Consequently, the
395 formation of TiO_2-MWCNT hybrid reduced the adsorption of proteins, which can be
396 attributed to the binding of the TiO_2 to the sites used in the protein's interaction with
397 MWCNT.

398

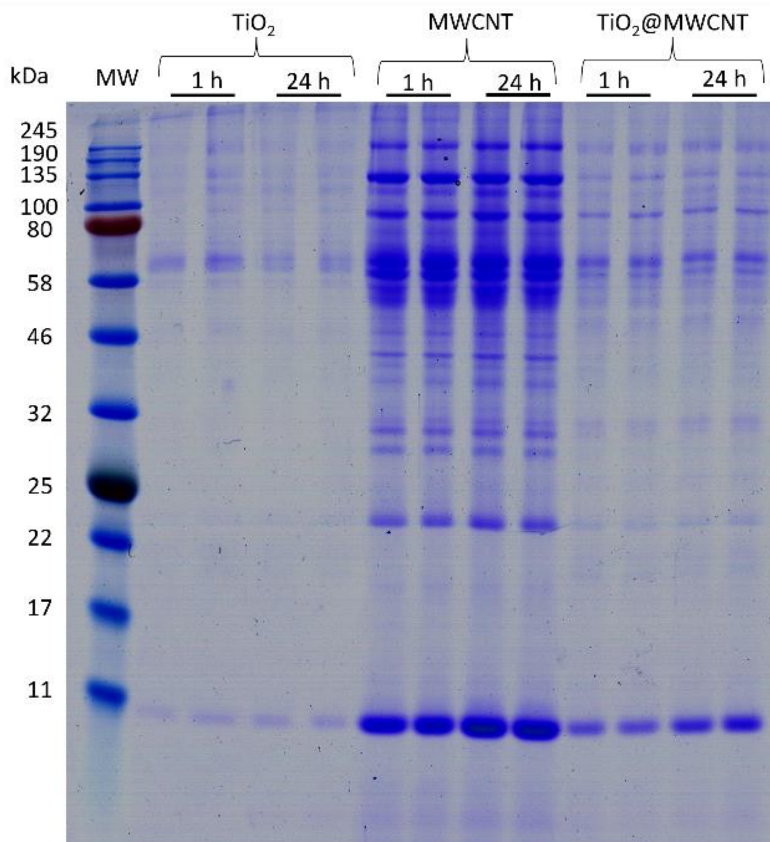

399

400 **Figure 3.** Biochemical characterisation of FBS hard corona associated with TiO_2,
401 MWCNT and TiO_2-MWCNT after incubation of 100 mg L^{-1} of each NM in DMEM with
402 10% FBS for 1 and 24 hours at 22 °C. MW = molecular weight of protein standard,
403 ranging from 11-245 kDa.

404

405 Overall, TiO_2-MWCNT did not elicit cytotoxic responses either with or without
406 FBS, at a concentration ranging from 0 to 100 μg mL^{-1}, after 24 hours of exposure, as
407 monitored by the alamar blue, neutral red and trypan blue assays (Figure 4). David et al.
408 (2022) also studied the cytotoxicity of TiO_2-MWCNT, in their studies the results showed
409 that cellulose acetate-collagen films containing 0.05 g of TiO_2-MWCNT nanoparticles
410 enhanced HDFn cell proliferation at 48 hours of exposure, this material also showed good
411 antimicrobial propriety being an excellent candidate to be applied in biomedical
412 technologies. Cendrowski et al. (2014), however, studying the effect of TiO_2-MWCNT
413 on mouse fibroblasts and human liver cells (0 to 100 μg mL^{-1}), observed that
414 concentrations greater than 25 μg mL^{-1} caused a decrease in cell viability after 24 hours
415 of exposure. However, the material studied by these authors differed in TiO_2 percentage
416 (19%) and TiO_2 crystallinity (anatase). In comparison, our material was composed of
417 approximately 70% of a mixture of rutile and anatase forms of TiO_2 NPs (20 and 80%,

respectively) (Da Silva et al., 2018). TiO_2 toxicity can be dependent of many characteristics, such as size, morphology, crystallinity (Cai et al., 2011; Gea et al., 2019; Uboldi et al., 2016; Wang and Fan, 2014). For example, Uboldi et al. (2016) studied the cytotoxicity of TiO_2 and found that anatase caused a significantly higher internalisation of anatase TiO_2 NPs in Balb/3T3 fibroblast, while rutile crystalline form induced more cytotoxicity, genotoxicity, and morphological transformation in both cell lines. The same can be said for MWCNT (Hamilton et al., 2013; Kyriakidou et al., 2020; Zhang et al., 2012; Zhou et al., 2017), depending on diameter, length and functional groups. For example, Zhou et al. (2017) studied the cytotoxicity and genotoxicity of pristine and functionalised (-OH and -COOH) MWCNT and observed that even though pristine MWCN caused more cell death, functionalised MWCNT were more genotoxic, besides the presence of BSA on culture media increase cytotoxicity for all materials. Those studies reinforced the dependence of material physical and chemical characteristics in the toxicological profile of nanomaterials.

It is important to notice that after 24 hours of exposure to TiO_2-MWCNT an increase in cell proliferation was observed by AB viability test. Two effects could be occurring, the NM can be stimulating cell metabolism or cell proliferation. Several reports sustain that TiO_2 NPs are biocompatible with cells, with a few reporting an enhancement in cell proliferation. For example, Vijayalakshmi et al. (2015) studied the cytotoxicity of TiO_2 NPs on MG63 cell line and observed that for concentrations up to 100 mg L^{-1}, TiO_2 NPs improved cell viability, causing cell proliferation when cells were exposed for 24 and 48 hours. The same was observed by Sun et al., (2016), their studies have shown that TiO_2-PEG NPs (<100 mg L^{-1}) can increase cell proliferation for HepG2 cells by increasing cell population in the S phase of cell cycle, they also showed that this NPs could aggregate hepatocyte growth factor receptors on the surface of cells which promote cell proliferation. However, these results are not always consistent, as some studies demonstrated that TiO_2 NPs can induce cell cycle arrest, decreasing cell proliferation. This was observed by Chang et al. (2022), who, through a systematic review and meta-analysis of 33 studies, concluded that TiO_2 NPs cause an increased percentage of cells in the sub-G1 phase, consequently causing cell cycle arrest.

For MWCNT, the results also are controversial as few studies also showed that MWCNT can cause cell proliferation, inducing cell cycle aberrations (Mihalchik et al., 2015a; Siegrist et al., 2014), while others showed that they could cause cell growth

451 inhibitions and cell cycle arrest (Ding et al., 2005; Zhang et al., 2011a). For example,
452 nitrogen-doped MWCNT causes proliferation in SAEC cells exposed for 24 hours to
453 concentrations up to 120 mg L^{-1}, they also observed an increase in the G2 phase of the
454 cell cycle (Mihalchik et al., 2015b). Similarly, Siegrist et al. (2014) observed that
455 carboxylated MWCNT caused proliferation on BEAS-2B cell line when exposed to
456 concentrations up to 2.4 μg cm^{-2} for 72 hours, they also observed a significant increase in
457 the S phase when cells were exposed to 24 μg cm^{-2} of carboxylated MWCNT for 24 hours.
458 Zhang et al. (2011) (Zhang et al., 2011b), however, observed that MWCNT cause a dose-
459 dependent decrease in 3T3 cells and human dermal fibroblast viability, which can be
460 related to the dose-dependent increase of cells in the G1 phase and fewer cells in the S
461 and G2/M phase. Similarly, Morozesk at al. (2020) observed that oxidised MWCNT
462 disturb the cell cycle, causing a reduction of cells in the G2/M phase, indicating a G1/S
463 phase block.

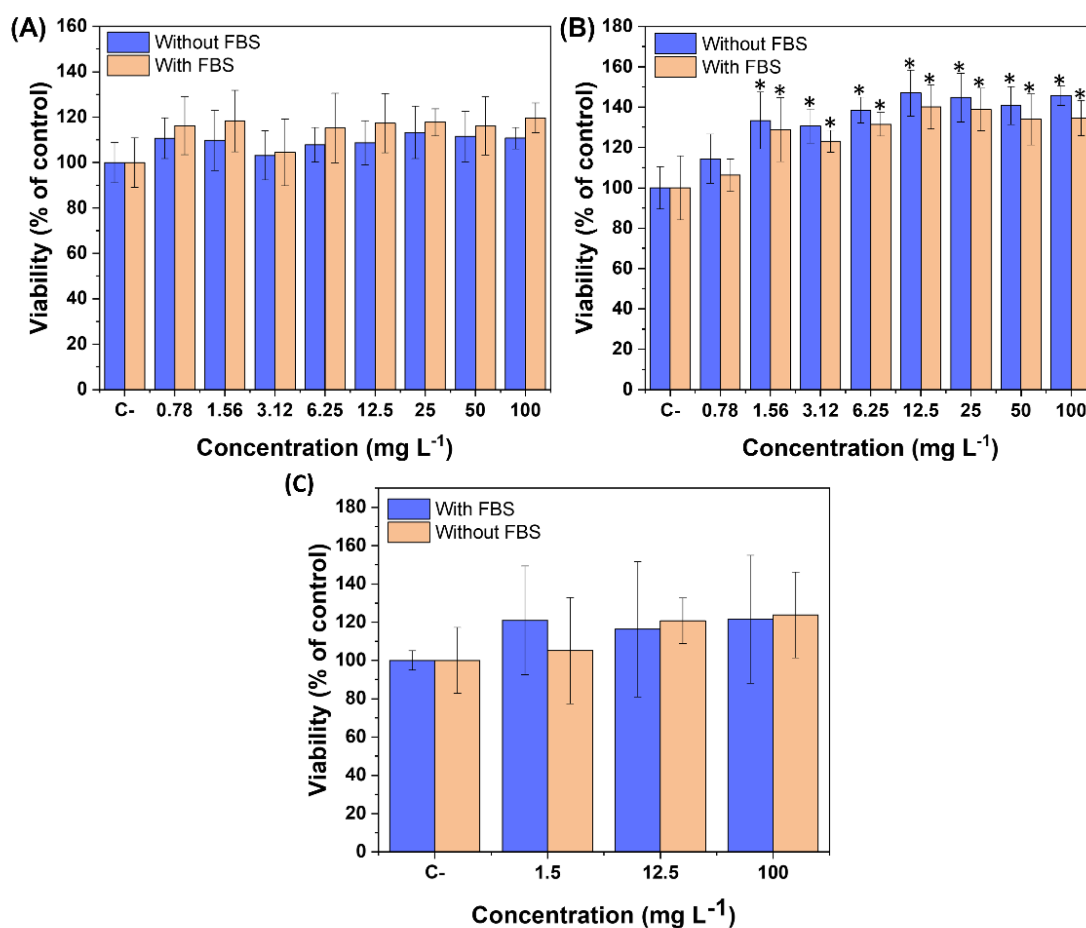

464

465 **Figure 4.** (A) Neutral red, (B) Alamar blue and (C) Trypan blue cell viability assay with
466 RTG-2 cell line exposed to TiO_2-MWCNT for 24 hours. Mean ± SEM of three individual

467 experiments. Data were analysed by one-way analysis of variance (ANOVA) and post
468 hoc comparisons of mean done by Dunnett's test ($P < 0.05$).

469

470 To analyse if the proliferation observed from alamar blue cell viability test was
471 due to cell cycle disruptions, we also performed a cell cycle cytometric flow analysis.
472 Initially, three concentrations were selected for the assay; 1, 10 and 100 mg L^{-1}, although
473 it was only possible to analyse 1 mg L^{-1}. For concentrations of 10 and 100 mg L^{-1}, the
474 NM was seen to be adhered to the cells, forming large aggregates, clogging the instrument
475 and preventing the analysis. No significant results were observed for treatment with FBS
476 compared to the control (Figure 5A). However, a significantly increased G2/M phase of
477 cell division was observed for the treatment without FBS (Figure 5B). In this sense, we
478 hypothesised that cell proliferation occurs in the exposure without FBS supplementation,
479 while an increase in metabolic activity occurs in the exposure with FBS supplementation.
480 Nanomaterials have the ability to increase cell metabolism resulting in a higher signal in
481 metabolic assays, such as AB and MTT (Longhin et al., 2022). This was observed, for
482 example, by Huang et al. (2009), where a time-dependent increase in MTT signal was
483 obtained when NIH 3T3 and HFW cells were exposed to 50 mg L^{-1} of TiO_2 NP. Similarly,
484 Machado et al. (2019), when studying the toxicity of hydroxyapatite nanoparticles by
485 MTT assay, observed an increase in HDFn cells metabolism after 48 hours of exposure
486 to 320 mg L^{-1} of NP. Dhenge et al. (2020) also observed a higher MTT signal, indicating
487 an increase in metabolism for WJ-MSCs cells exposed to 25 and 10 mg L^{-1} of hybrid
488 graphene oxide.

489

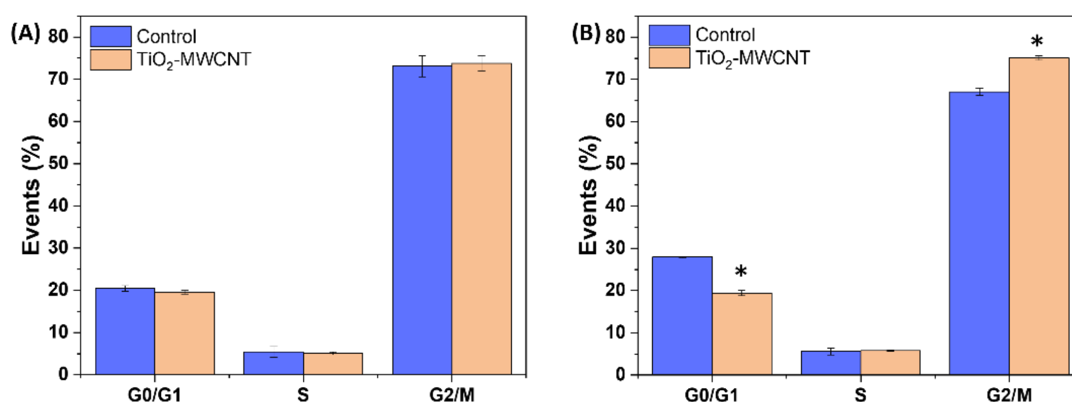

490

491 **Figure 5.** Cell cycle cytometric flow assay with RTG-2 exposed to 1 mg L^{-1} of TiO_2-
492 MWCNT for 24 hours (A) with and (B) without FBS in DMEM media. Mean ± SEM of

493 three individual experiments. Data were analysed by one-way analysis of variance
494 (ANOVA), post hoc comparison of mean done by Dunnett's test (* = $P < 0.05$).

495

496 The interaction between nanomaterials and RTG-2 cells was analysed by
497 enhanced dark-field hyperspectral microscopy (CytoViva). Figure 6 A and B show
498 hyperspectral images of the mapped RTG-2 cell, in which the red dots represent the pixels
499 where TiO_2-MWCNT spectra were found. It was observed that, even after several
500 washing steps, NP was still attached to the cell membrane. Hence, to analyse if NP were
501 being internalised, Confocal Raman spectroscopy was applied. Measurements in the Z
502 axis (depth) were used to detect the internalisation of the nanomaterials through the
503 intensity of the MWNT D and G bands measured when translating along the Z axis (1 μm
504 steps) (Alnasser et al., 2019). We can observe that, for TiO_2-MWCNT treated with FBS
505 (Figure 6G), the intensity of the D and G bands was consistently larger inside the cells
506 and that this intensity decreases at the extremes of the Z axis (top and bottom of the cell),
507 proving that the nanomaterial was present inside the cell. In the absence of FBS, the
508 intensity of the D and G bands was highest at the top of the cells but decreased
509 monotonically along the Z axis. Therefore, without FBS, TiO_2-MWCNT tended to
510 aggregate and adhere to the cell membrane. Studies suggested that protein corona can
511 promote nanoparticle uptake. For example, Posati et al. (2012) studied the effect of bovine
512 serum albumin (BSA) in the internalisation of ZnAl-HTlc NP on MDCK and HeLa cell
513 lines and observed that in the presence of BSA the NM was internalised. However, no
514 internalisation was observed in the absence of BSA. For TiO_2 NPs, Tedja et al. (2012)
515 studied the uptake profile of TiO_2 NPs in the presence and absence of serum and observed
516 that in the presence of FBS the uptake of TiO_2 NPs was higher than in non-FBS treated
517 TiO_2 NPs. These results were also observed by Vranic et al. (2017) where TiO_2 NPs in
518 the presence of bovine serum were more efficiently internalised. In the case of MWCNT,
519 Long et al. (2018b) observed that pre-incubation on MWCNT with BSA, forming a
520 protein corona, enhances the internalisation of this material to HUVEC cells. Similarly,
521 Zhang et al. (2019) observed that protein corona-coated pristine MWCNT were more
522 internalised than uncoated pristine MWCNT.

523 Considering the above, only a limited information is available about the
524 cytotoxicity and internalisation of TiO_2@MWCNT. Hence, this study provides an
525 important contribution towards the toxicological evaluation of TiO_2@MWCNT

nanohybrid materials. Further, it can serve as a starting point to understand how protein corona can influence the interaction between nanohybrid materials and cells.

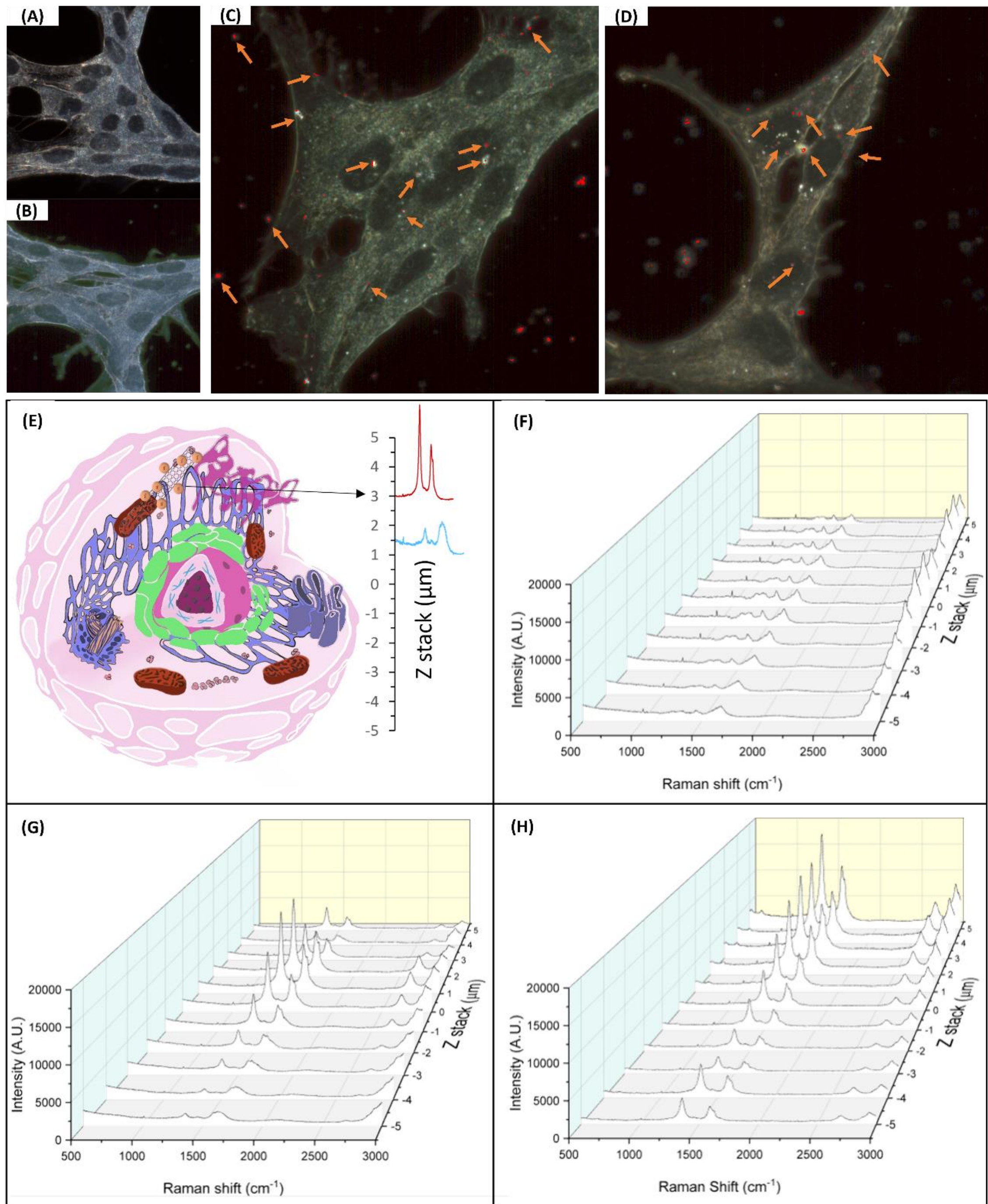

Figure 6. A to D show hyperspectral images of cells (RTG-2) treated with 1 mg L^{-1} of TiO_2-MWCNT; (A) Control cells in DMEM with FBS; (B) Control cells in DMEM without FBS; (C) TiO_2-MWCNT in DMEM media with FBS and (D) TiO_2-MWCNT without FBS. Red dots indicate the location of the nanomaterial in the cells (Point by the orange arrows. Images captured with 100x objective. E-H shows Raman spectral analysis of RTG-2 cells treated with 1 mg L^{-1} of TiO_2-MWCNT; (E) Cell representation of the Raman spectra analysis, where cell was divided in 10 um and laser capture Raman spectra every 1 um step. (F) Z-axis intensity map of a control cell, (G) cell exposed to TiO_2-

MWCNT with SFB and (H) without SFB. Bands used for the map: 1350 cm^{-1} for the D-band and 1580 cm^{-1} for the G-band.

4. Conclusion

In summary, *in vitro* assays with the RTG-2 cell line showed absence of toxicity to TiO_2-MWCNT nanohybrid up to 100 mg mL^{-1}. Furthermore, it was observed that FBS-protein corona on TiO_2-MWCNT had a different profile when compared to MWCNT and TiO_2 nanoparticles. Cryo-TEM images confirmed that TiO_2 has attached to the nanotube surface after incubation with cell culture medium and FBS-protein corona formation. Exploring two complementary advanced optical microscopy techniques (CytoViva and Raman), it was possible to observe that this nanohybrid adheres to the cell membrane in the presence and absence of FBS in the culture medium. The internalisation of nanohybrid was evident when coated with FBS proteins. Finally, this study showed the potential of the RTG-2 cell line as a convenient model for a screening approach for hazards and given the current interest in TiO_2-MWCNT for a range of novel applications, we highlight the potential for this material, as it indicates low toxicity, based on short-term cellular viability test.

Declaration of Competing Interest

The authors declare that they have no known competing financial interests or personal relationships that could have appeared to influence the work reported in this paper.

Acknowledgments

The authors are grateful to the financial support of the Government of Ireland International Education Scholarship (GOI-IES), the National Council for Scientific and Technological Development (CNPq) and for the Coordenação de Aperfeiçoamento de Pessoal de Nível Superior (CAPES/Brasil) finance code 001, INCT-Inomat, and National System of Laboratories on Nanotechnologies (SisNANO/MCTIC). The authors also thank the CNPEM open-facilities (Cryo-TEM and NANOTOX) for the research support.

References

569 Abbas, N., Shao, G.N., Haider, M.S., Imran, S.M., Park, S.S., Jeon, S.-J., Kim, H.T.,
570 2016. Inexpensive sol-gel synthesis of multiwalled carbon nanotube-TiO2 hybrids
571 for high performance antibacterial materials. Materials Science and Engineering: C
572 68, 780–788. https://doi.org/10.1016/j.msec.2016.07.036

573 Ahmadi, M., Ramezani Motlagh, H., Jaafarzadeh, N., Mostoufi, A., Saeedi, R.,
574 Barzegar, G., Jorfi, S., 2017. Enhanced photocatalytic degradation of tetracycline
575 and real pharmaceutical wastewater using MWCNT/TiO2 nano-composite. J
576 Environ Manage 186, 55–63. https://doi.org/10.1016/j.jenvman.2016.09.088

577 Allegri, M., Perivoliotis, D.K., Bianchi, M.G., Chiu, M., Pagliaro, A., Koklioti, M.A.,
578 Trompeta, A.-F.A., Bergamaschi, E., Bussolati, O., Charitidis, C.A., 2016.
579 Toxicity determinants of multi-walled carbon nanotubes: The relationship between
580 functionalization and agglomeration. Toxicol Rep 3, 230–243.
581 https://doi.org/10.1016/J.TOXREP.2016.01.011

582 Alnasser, F., Castagnola, V., Boselli, L., Esquivel-Gaon, M., Efeoglu, E., McIntyre, J.,
583 Byrne, H.J., Dawson, K.A., 2019. Graphene Nanoflake Uptake Mediated by
584 Scavenger Receptors. Nano Lett 19, 1260–1268.
585 https://doi.org/10.1021/acs.nanolett.8b04820

586 Belkhanchi, H., Ziat, Y., Hammi, M., Laghlimi, C., Moutcine, A., Benyounes, A.,
587 Kzaiber, F., 2021. Nitrogen doped carbon nanotubes grafted TiO2 rutile nanofilms:
588 Promising material for dye sensitized solar cell application. Optik (Stuttg) 229,
589 166234. https://doi.org/10.1016/j.ijleo.2020.166234

590 Belkhanchi, H., Ziat, Y., Hammi, M., Laghlimi, C., Moutcine, A., Benyounes, A.,
591 Kzaiber, F., 2020. Synthesis of N-CNT/TiO 2 composites thin films: surface
592 analysis and optoelectronic properties. E3S Web of Conferences 183, 05002.
593 https://doi.org/10.1051/e3sconf/202018305002

594 Bermejo-Nogales, A., Fernández-Cruz, M.L., Navas, J.M., 2017. Fish cell lines as a tool
595 for the ecotoxicity assessment and ranking of engineered nanomaterials.
596 Regulatory Toxicology and Pharmacology 90, 297–307.
597 https://doi.org/10.1016/j.yrtph.2017.09.029

598 Bols, N.C., Dayeh, V.R., Lee, L.E.J., Schirmer, K., 2005. Chapter 2 Use of fish cell
599 lines in the toxicology and ecotoxicology of fish. Piscine cell lines in
600 environmental toxicology, in: Biochemistry and Molecular Biology of Fishes. pp.
601 43–84. https://doi.org/10.1016/S1873-0140(05)80005-0

602 Borgognoni, C.F., Mormann, M., Qu, Y., Schäfer, M., Langer, K., Öztürk, C., Wagner,
603 S., Chen, C., Zhao, Y., Fuchs, H., Riehemann, K., 2015. Reaction of human
604 macrophages on protein corona covered TiO2 nanoparticles. Nanomedicine 11,
605 275–282. https://doi.org/10.1016/J.NANO.2014.10.001

606 Breznan, D., Das, D., MacKinnon-Roy, C., Simard, B., Kumarathasan, P., Vincent, R.,
607 2015. Non-specific interaction of carbon nanotubes with the resazurin assay
608 reagent: Impact on in vitro assessment of nanoparticle cytotoxicity. Toxicology in
609 Vitro 29, 142–147. https://doi.org/10.1016/J.TIV.2014.09.009

610 Cai, K., Hou, Y., Hu, Y., Zhao, L., Luo, Z., Shi, Y., Lai, M., Yang, W., Liu, P., 2011.
611 Correlation of the Cytotoxicity of TiO2 Nanoparticles with Different Particle Sizes
612 on a Sub-200-nm Scale. Small 7, 3026–3031.
613 https://doi.org/10.1002/smll.201101170

614 Casado, M., Macken, A., Byrne, H., 2013. Ecotoxicological assessment of silica and
615 polystyrene nanoparticles assessed by a multitrophic test battery. Environ Int.

616 Casey, A., Herzog, E., Davoren, M., Lyng, F.M., Byrne, H.J., Chambers, G., 2007.
617 Spectroscopic analysis confirms the interactions between single walled carbon
618 nanotubes and various dyes commonly used to assess cytotoxicity. Carbon N Y 45,
619 1425–1432. https://doi.org/10.1016/J.CARBON.2007.03.033

620 Castaño, A., Cantarino, M.J., Castillo, P., Tarazona, J.V., 1996. Correlations between
621 the RTG-2 cytotoxicity test EC50 and in vivo LC50 rainbow trout bioassay.
622 Chemosphere 32, 2141–2157. https://doi.org/10.1016/0045-6535(96)00126-9

623 Cendrowski, K., Jedrzejczak, M., Peruzynska, M., Dybus, A., Drozdzik, M., Mijowska,
624 E., 2014. Preliminary study towards photoactivity enhancement using a
625 biocompatible titanium dioxide/carbon nanotubes composite. J Alloys Compd 605,
626 173–178. https://doi.org/10.1016/j.jallcom.2014.03.112

627 Chang, H., Wang, Q., Meng, X., Chen, X., Deng, Y., Li, L., Yang, Y., Song, G., Jia, H.,
628 2022. Effect of Titanium Dioxide Nanoparticles on Mammalian Cell Cycle *In*
629 *Vitro* : A Systematic Review and Meta-Analysis. Chem Res Toxicol 35, 1435–
630 1456. https://doi.org/10.1021/acs.chemrestox.1c00402

631 Chen, H., Yang, S., Yu, K., Ju, Y., Sun, C., 2011. Effective Photocatalytic Degradation
632 of Atrazine over Titania-Coated Carbon Nanotubes (CNTs) Coupled with
633 Microwave Energy. J Phys Chem A 115, 3034–3041.
634 https://doi.org/10.1021/jp109948n

635 Chen, R., Lan, G., Wang, N., Yan, W., Yi, J., Wei, W., 2022. Highly sensitive fiber-
636 optic SPR sensor with surface coated TiO_2 /MWCNT composite film for hydrogen
637 sulfide gas detection. J Phys D Appl Phys 55, 105108.
638 https://doi.org/10.1088/1361-6463/ac378f

639 da Cruz Schneid, A., Albuquerque, L.J.C., Mondo, G.B., Ceolin, M., Picco, A.S.,
640 Cardoso, M.B., 2022. Colloidal stability and degradability of silica nanoparticles in
641 biological fluids: a review. J Solgel Sci Technol. https://doi.org/10.1007/s10971-
642 021-05695-8

643 Da Dalt, S., Alves, A.K., Bergmann, C.P., 2013. Photocatalytic degradation of methyl
644 orange dye in water solutions in the presence of MWCNT/TiO2 composites. Mater
645 Res Bull 48, 1845–1850. https://doi.org/10.1016/j.materresbull.2013.01.022

646 Da Silva, G.H., Clemente, Z., Khan, L.U., Coa, F., Neto, L.L.R., Carvalho, H.W.P.,
647 Castro, V.L., Martinez, D.S.T., Monteiro, R.T.R., 2018. Toxicity assessment of
648 TiO2-MWCNT nanohybrid material with enhanced photocatalytic activity on
649 Danio rerio (Zebrafish) embryos. Ecotoxicol Environ Saf 165, 136–143.
650 https://doi.org/10.1016/j.ecoenv.2018.08.093

651 Darbari, S., Abdi, Y., Haghighi, F., Mohajerzadeh, S., Haghighi, N., 2011. Investigating
652 the antifungal activity of TiO 2 nanoparticles deposited on branched carbon
653 nanotube arrays. J Phys D Appl Phys 44, 245401. https://doi.org/10.1088/0022-
654 3727/44/24/245401

655 Das, D., Sabaraya, I.V., Zhu, T., Sabo-Attwood, T., Saleh, N.B., 2018. Aggregation
656 Behavior of Multiwalled Carbon Nanotube-Titanium Dioxide Nanohybrids:
657 Probing the Part-Whole Question. Environ Sci Technol 52, 8233–8241.
658 https://doi.org/10.1021/acs.est.7b05826

659 Das, S., Chakraborty, K., Ghosh, D., Pulimi, M., Chandrasekaran, N., Anand, S., Rai,
660 P.K., Mukherjee, A., 2022. Systematic assessment of f-MWCNT transport in
661 aqueous medium: the effect of shear and non-shear forces. International Journal of
662 Environmental Science and Technology. https://doi.org/10.1007/s13762-022-
663 04295-5

664 David, M.E., Ion, R.M., Grigorescu, R.M., Iancu, L., Holban, A.M., Iordache, F.,
665 Nicoara, A.I., Alexandrescu, E., Somoghi, R., Teodorescu, S., Gheboianu, A.I.,
666 2022. Biocompatible and Antimicrobial Cellulose Acetate-Collagen Films
667 Containing MWCNTs Decorated with TiO2 Nanoparticles for Potential
668 Biomedical Applications. Nanomaterials 12, 239.
669 https://doi.org/10.3390/nano12020239

670 de Medeiros, A.M.Z., Khan, L.U., da Silva, G.H., Ospina, C.A., Alves, O.L., de Castro,
671 V.L., Martinez, D.S.T., 2021. Graphene oxide-silver nanoparticle hybrid material:
672 an integrated nanosafety study in zebrafish embryos. Ecotoxicol Environ Saf 209,
673 111776. https://doi.org/10.1016/j.ecoenv.2020.111776

674 Dhenge, S.A., Gade, N.E., Mishra, O.P., Kumar, A., Khandait, V.N., 2020. In vitro
675 Cytotoxicity Analysis of Hybrid Graphene Oxide (hGO) Nano Structures in
676 Caprine Wharton's Jelly Derived Mesenchymal Stem Cells (WJ-MSCs). Indian J
677 Anim Res. https://doi.org/10.18805/ijar.B-3992

678 Di Ianni, E., Erdem, J.S., Møller, P., Sahlgren, N.M., Poulsen, S.S., Knudsen, K.B.,
679 Zienolddiny, S., Saber, A.T., Wallin, H., Vogel, U., Jacobsen, N.R., 2021. In vitro-
680 in vivo correlations of pulmonary inflammogenicity and genotoxicity of MWCNT.
681 Part Fibre Toxicol 18, 25. https://doi.org/10.1186/s12989-021-00413-2

682 Ding, L., Stilwell, J., Zhang, T., Elboudwarej, O., Jiang, H., Selegue, J.P., Cooke, P.A.,
683 Gray, J.W., Chen, F.F., 2005. Molecular Characterization of the Cytotoxic
684 Mechanism of Multiwall Carbon Nanotubes and Nano-Onions on Human Skin
685 Fibroblast. Nano Lett 5, 2448–2464. https://doi.org/10.1021/nl051748o

686 Docter, D., Distler, U., Storck, W., Kuharev, J., Wünsch, D., Hahlbrock, A., Knauer,
687 S.K., Tenzer, S., Stauber, R.H., 2014. Quantitative profiling of the protein coronas
688 that form around nanoparticles. Nat Protoc 9, 2030–2044.
689 https://doi.org/10.1038/nprot.2014.139

690 Du, P., Zhao, J., Mashayekhi, H., Xing, B., 2014. Adsorption of Bovine Serum Albumin
691 and Lysozyme on Functionalized Carbon Nanotubes. The Journal of Physical
692 Chemistry C 118, 22249–22257. https://doi.org/10.1021/jp5044943

Fent, K., 2001. Fish cell lines as versatile tools in ecotoxicology: assessment of cytotoxicity, cytochrome P4501A induction potential and estrogenic activity of chemicals and environmental samples. Toxicology in Vitro 15, 477–488. https://doi.org/10.1016/S0887-2333(01)00053-4

Forest, V., 2022. Experimental and Computational Nanotoxicology—Complementary Approaches for Nanomaterial Hazard Assessment. Nanomaterials 12, 1346. https://doi.org/10.3390/nano12081346

Franqui, L.S., De Farias, M.A., Portugal, R. V., Costa, C.A.R., Domingues, R.R., Souza Filho, A.G., Coluci, V.R., Leme, A.F.P., Martinez, D.S.T., 2019. Interaction of graphene oxide with cell culture medium: Evaluating the fetal bovine serum protein corona formation towards in vitro nanotoxicity assessment and nanobiointeractions. Materials Science and Engineering: C 100, 363–377. https://doi.org/10.1016/J.MSEC.2019.02.066

Galbis-Martínez, L., Fernández-Cruz, M.L., Alte, L., Valdehita, A., Rucandio, I., Navas, J.M., 2018. Development of a new tool for the long term in vitro ecotoxicity testing of nanomaterials using a rainbow-trout cell line (RTL-W1). Toxicology in Vitro 50, 305–317. https://doi.org/10.1016/J.TIV.2018.04.007

Garvas, M., Testen, A., Umek, P., Gloter, A., Koklic, T., Strancar, J., 2015. Protein Corona Prevents TiO2 Phototoxicity. PLoS One 10, e0129577. https://doi.org/10.1371/journal.pone.0129577

Gea, M., Bonetta, Sara, Iannarelli, L., Giovannozzi, A.M., Maurino, V., Bonetta, Silvia, Hodoroaba, V.-D., Armato, C., Rossi, A.M., Schilirò, T., 2019. Shape-engineered titanium dioxide nanoparticles (TiO2-NPs): cytotoxicity and genotoxicity in bronchial epithelial cells. Food and Chemical Toxicology 127, 89–100. https://doi.org/10.1016/j.fct.2019.02.043

Ghartavol, H.M., Mohammadi, M.R., Afshar, A., Li, Y., 2019. On the assessment of incorporation of CNT–TiO 2 core–shell structures into nanoparticle TiO 2 photoanodes in dye-sensitized solar cells. Photochemical & Photobiological Sciences 18, 1840–1850. https://doi.org/10.1039/C9PP00100J

Goswami, M., Yashwanth, B.S., Trudeau, V., Lakra, W.S., 2022. Role and relevance of fish cell lines in advanced in vitro research. Mol Biol Rep 49, 2393–2411. https://doi.org/10.1007/s11033-021-06997-4

Guler, M.O., Cetinkaya, T., Uysal, M., Akbulut, H., 2015. High efficiency TiO$_2$ /MWCNT based anode electrodes for Li-ion batteries. Int J Energy Res 39, 172–180. https://doi.org/10.1002/er.3220

Hamid, S.B.A., Tan, T.L., Lai, C.W., Samsudin, E.M., 2014. Multiwalled carbon nanotube/TiO2 nanocomposite as a highly active photocatalyst for photodegradation of Reactive Black 5 dye. Chinese Journal of Catalysis 35, 2014–2019. https://doi.org/10.1016/S1872-2067(14)60210-2

Hamilton, R.F., Wu, Z., Mitra, S., Shaw, P.K., Holian, A., 2013. Effect of MWCNT size, carboxylation, and purification on in vitro and in vivo toxicity, inflammation

734 and lung pathology. Part Fibre Toxicol 10, 57. https://doi.org/10.1186/1743-8977-
735 10-57

736 Hemalatha, K., Ette, P.M., Madras, G., Ramesha, K., 2015. Visible light assisted
737 photocatalytic degradation of organic dyes on TiO2–CNT nanocomposites. J
738 Solgel Sci Technol 73, 72–82. https://doi.org/10.1007/s10971-014-3496-0

739 Hernández-Alonso, M.D., Fresno, F., Suárez, S., Coronado, J.M., 2009. Development of
740 alternative photocatalysts to TiO2: Challenges and opportunities. Energy Environ
741 Sci 2, 1231. https://doi.org/10.1039/b907933e

742 Hernández-Moreno, D., Blázquez, M., Navas, J., Fernández-Cruz, M., 2022. Fish cell
743 lines as screening tools to predict acute toxicity to fish of biocidal active
744 substances and their relevant environmental metabolites. Aquatic Toxicology 242,
745 106020. https://doi.org/10.1016/j.aquatox.2021.106020

746 Huang, S., Chueh, P.J., Lin, Y.-W., Shih, T.-S., Chuang, S.-M., 2009. Disturbed mitotic
747 progression and genome segregation are involved in cell transformation mediated
748 by nano-TiO2 long-term exposure. Toxicol Appl Pharmacol 241, 182–194.
749 https://doi.org/10.1016/j.taap.2009.08.013

750 Jones, C.F., Grainger, D.W., 2009. In vitro assessments of nanomaterial toxicity. Adv
751 Drug Deliv Rev 61, 438–456. https://doi.org/10.1016/j.addr.2009.03.005

752 Klingelfus, T., Disner, G.R., Voigt, C.L., Alle, L.F., Cestari, M.M., Leme, D.M., 2019.
753 Nanomaterials induce DNA-protein crosslink and DNA oxidation: A mechanistic
754 study with RTG-2 fish cell line and Comet assay modifications. Chemosphere 215,
755 703–709. https://doi.org/10.1016/j.chemosphere.2018.10.118

756 Kolarova, J., Velisek, J., Svobodova, Z., 2021. Comparison of in vitro (fish cell line)
757 and in vivo (fish and crustacean) acute toxicity tests in aquatic toxicology. Vet
758 Med (Praha) 66, 350–355. https://doi.org/10.17221/161/2020-VETMED

759 Kyriakidou, K., Brasinika, D., Trompeta, A.F.A., Bergamaschi, E., Karoussis, I.K.,
760 Charitidis, C.A., 2020. In vitro cytotoxicity assessment of pristine and carboxyl-
761 functionalized MWCNTs. Food and Chemical Toxicology 141, 111374.
762 https://doi.org/10.1016/j.fct.2020.111374

763 Lee, T.Y., Alegaonkar, P.S., Yoo, J.-B., 2007. Fabrication of dye sensitized solar cell
764 using TiO2 coated carbon nanotubes. Thin Solid Films 515, 5131–5135.
765 https://doi.org/10.1016/j.tsf.2006.10.056

766 Lesniak, A., Fenaroli, F., Monopoli, M.P., Åberg, C., Dawson, K.A., Salvati, A., 2012.
767 Effects of the Presence or Absence of a Protein Corona on Silica Nanoparticle
768 Uptake and Impact on Cells. ACS Nano 6, 5845–5857.
769 https://doi.org/10.1021/nn300223w

770 Long, J., Li, X., Kang, Y., Ding, Y., Gu, Z., Cao, Y., 2018a. Internalization,
771 cytotoxicity, oxidative stress and inflammation of multi-walled carbon nanotubes
772 in human endothelial cells: Influence of pre-incubation with bovine serum
773 albumin. RSC Adv 8, 9253–9260. https://doi.org/10.1039/c8ra00445e

774 Long, J., Li, X., Kang, Y., Ding, Y., Gu, Z., Cao, Y., 2018b. Internalization,
775 cytotoxicity, oxidative stress and inflammation of multi-walled carbon nanotubes
776 in human endothelial cells: influence of pre-incubation with bovine serum albumin.
777 RSC Adv 8, 9253–9260. https://doi.org/10.1039/C8RA00445E

778 Longhin, E.M., el Yamani, N., Rundén-Pran, E., Dusinska, M., 2022. The alamar blue
779 assay in the context of safety testing of nanomaterials. Frontiers in Toxicology 4.
780 https://doi.org/10.3389/ftox.2022.981701

781 Lundqvist, M., Stigler, J., Cedervall, T., Berggård, T., Flanagan, M.B., Lynch, I., Elia,
782 G., Dawson, K., 2011. The Evolution of the Protein Corona around Nanoparticles:
783 A Test Study. ACS Nano 5, 7503–7509. https://doi.org/10.1021/nn202458g

784 Lungu-Mitea, S., Oskarsson, A., Lundqvist, J., 2018. Development of an oxidative
785 stress in vitro assay in zebrafish (Danio rerio) cell lines. Sci Rep 8, 12380.
786 https://doi.org/10.1038/s41598-018-30880-1

787 Machado, T.R., Leite, I.S., Inada, N.M., Li, M.S., da Silva, J.S., Andrés, J., Beltrán-Mir,
788 H., Cordoncillo, E., Longo, E., 2019. Designing biocompatible and multicolor
789 fluorescent hydroxyapatite nanoparticles for cell-imaging applications. Mater
790 Today Chem 14, 100211. https://doi.org/10.1016/j.mtchem.2019.100211

791 Martinez, D.S.T., Da Silva, G.H., de Medeiros, A.M.Z., Khan, L.U., Papadiamantis,
792 A.G., Lynch, I., 2020. Effect of the Albumin Corona on the Toxicity of Combined
793 Graphene Oxide and Cadmium to Daphnia magna and Integration of the Datasets
794 into the NanoCommons Knowledge Base. Nanomaterials 10, 1936.
795 https://doi.org/10.3390/nano10101936

796 Martins, C.H.Z., Côa, F., da Silva, G.H., Bettini, J., de Farias, M.A., Portugal, R.V.,
797 Umbuzeiro, G. de A., Alves, O.L., Martinez, D.S.T., 2022. Functionalization of
798 carbon nanotubes with bovine plasma biowaste by forming a protein corona
799 enhances copper removal from water and ecotoxicity mitigation. Environ Sci Nano
800 9, 2887–2905. https://doi.org/10.1039/D2EN00145D

801 Mihalchik, A.L., Ding, W., Porter, D.W., McLoughlin, C., Schwegler-Berry, D., Sisler,
802 J.D., Stefaniak, A.B., Snyder-Talkington, B.N., Cruz-Silva, R., Terrones, M.,
803 Tsuruoka, S., Endo, M., Castranova, V., Qian, Y., 2015a. Effects of nitrogen-
804 doped multi-walled carbon nanotubes compared to pristine multi-walled carbon
805 nanotubes on human small airway epithelial cells. Toxicology 333, 25–36.
806 https://doi.org/10.1016/j.tox.2015.03.008

807 Mihalchik, A.L., Ding, W., Porter, D.W., McLoughlin, C., Schwegler-Berry, D., Sisler,
808 J.D., Stefaniak, A.B., Snyder-Talkington, B.N., Cruz-Silva, R., Terrones, M.,
809 Tsuruoka, S., Endo, M., Castranova, V., Qian, Y., 2015b. Effects of nitrogen-
810 doped multi-walled carbon nanotubes compared to pristine multi-walled carbon
811 nanotubes on human small airway epithelial cells. Toxicology 333, 25–36.
812 https://doi.org/10.1016/j.tox.2015.03.008

813 Mombeshora, E.T., Muchuweni, E., Davies, M.L., Nyamori, V.O., Martincigh, B.S.,
814 2022. Metal-organic chemical vapor deposition of anatase titania on multiwalled

815 carbon nanotubes for electrochemical capacitors. Energy Sci Eng.
816 https://doi.org/10.1002/ese3.1234

817 Monopoli, M.P., Åberg, C., Salvati, A., Dawson, K.A., 2012. Biomolecular coronas
818 provide the biological identity of nanosized materials. Nat Nanotechnol 7, 779–
819 786. https://doi.org/10.1038/nnano.2012.207

820 Morozesk, M., Franqui, L.S., Mansano, A.S., Martinez, D.S.T., Fernandes, M.N., 2018.
821 Interactions of oxidized multiwalled carbon nanotube with cadmium on zebrafish
822 cell line: The influence of two co-exposure protocols on in vitro toxicity tests.
823 Aquatic Toxicology 200, 136–147. https://doi.org/10.1016/j.aquatox.2018.05.002

824 Morozesk, M., Franqui, L.S., Pinheiro, F.C., Nóbrega, J.A., Martinez, D.S.T.,
825 Fernandes, M.N., 2020. Effects of multiwalled carbon nanotubes co-exposure with
826 cadmium on zebrafish cell line: Metal uptake and accumulation, oxidative stress,
827 genotoxicity and cell cycle. Ecotoxicol Environ Saf 202, 110892.
828 https://doi.org/10.1016/J.ECOENV.2020.110892

829 Muduli, S., Lee, W., Dhas, V., Mujawar, S., Dubey, M., Vijayamohanan, K., Han, S.-
830 H., Ogale, S., 2009. Enhanced Conversion Efficiency in Dye-Sensitized Solar
831 Cells Based on Hydrothermally Synthesized TiO_2 −MWCNT Nanocomposites.
832 ACS Appl Mater Interfaces 1, 2030–2035. https://doi.org/10.1021/am900396m

833 Munari, M., Sturve, J., Frenzilli, G., Sanders, M.B., Brunelli, A., Marcomini, A., Nigro,
834 M., Lyons, B.P., 2014. Genotoxic effects of CdS quantum dots and Ag 2 S
835 nanoparticles in fish cell lines (RTG-2). Mutation Research/Genetic Toxicology
836 and Environmental Mutagenesis 775–776, 89–93.
837 https://doi.org/10.1016/j.mrgentox.2014.09.003

838 Naha, P.C., Byrne, H.J., 2013. Generation of intracellular reactive oxygen species and
839 genotoxicity effect to exposure of nanosized polyamidoamine (PAMAM)
840 dendrimers in PLHC-1 cells in vitro. Aquatic Toxicology 132–133, 61–72.
841 https://doi.org/10.1016/j.aquatox.2013.01.020

842 Naha, P.C., Davoren, M., Casey, A., Byrne, H.J., 2009. An Ecotoxicological Study of
843 Poly(amidoamine) Dendrimers-Toward Quantitative Structure Activity
844 Relationships. Environ Sci Technol 43, 6864–6869.
845 https://doi.org/10.1021/es901017v

846 Nasr, M., Eid, C., Habchi, R., Miele, P., Bechelany, M., 2018. Recent Progress on
847 Titanium Dioxide Nanomaterials for Photocatalytic Applications. ChemSusChem
848 11, 3023–3047. https://doi.org/10.1002/cssc.201800874

849 Natarajan, L., Jenifer, M.A., Mukherjee, A., 2021. Eco-corona formation on the
850 nanomaterials in the aquatic systems lessens their toxic impact: A comprehensive
851 review. Environ Res 194, 110669. https://doi.org/10.1016/j.envres.2020.110669

852 Nel, A.E., Mädler, L., Velegol, D., Xia, T., Hoek, E.M. V., Somasundaran, P., Klaessig,
853 F., Castranova, V., Thompson, M., 2009. Understanding biophysicochemical
854 interactions at the nano–bio interface. Nat Mater 8, 543–557.
855 https://doi.org/10.1038/nmat2442

856 Olowoyo, J.O., Kumar, M., Jain, S.L., Babalola, J.O., Vorontsov, A. V., Kumar, U.,
857 2019. Insights into Reinforced Photocatalytic Activity of the CNT–TiO 2
858 Nanocomposite for CO 2 Reduction and Water Splitting. The Journal of Physical
859 Chemistry C 123, 367–378. https://doi.org/10.1021/acs.jpcc.8b07894

860 Orge, C.A., Soares, O.S.G.P., Faria, J.L., Pereira, M.F.R., 2017. Synthesis of TiO2-
861 Carbon Nanotubes through ball-milling method for mineralization of oxamic acid
862 (OMA) by photocatalytic ozonation. J Environ Chem Eng 5, 5599–5607.
863 https://doi.org/10.1016/J.JECE.2017.10.030

864 Parsai, T., Kumar, A., 2019. Understanding effect of solution chemistry on
865 heteroaggregation of zinc oxide and copper oxide nanoparticles. Chemosphere 235,
866 457–469. https://doi.org/10.1016/j.chemosphere.2019.06.171

867 Paula, A.J., Silveira, C.P., Martinez, D.S.T., Souza Filho, A.G., Romero, F. V.,
868 Fonseca, L.C., Tasic, L., Alves, O.L., Durán, N., 2014. Topography-driven
869 bionano-interactions on colloidal silica nanoparticles. ACS Appl Mater Interfaces
870 6, 3437–3447. https://doi.org/10.1021/am405594q

871 Petry, R., Saboia, V.M., Franqui, L.S., Holanda, C. de A., Garcia, T.R.R., de Farias,
872 M.A., de Souza Filho, A.G., Ferreira, O.P., Martinez, D.S.T., Paula, A.J., 2019. On
873 the formation of protein corona on colloidal nanoparticles stabilized by depletant
874 polymers. Materials Science and Engineering: C 105, 110080.
875 https://doi.org/10.1016/j.msec.2019.110080

876 Posati, T., Bellezza, F., Tarpani, L., Perni, S., Latterini, L., Marsili, V., Cipiciani, A.,
877 2012. Selective internalization of ZnAl-HTlc nanoparticles in normal and tumor
878 cells. A study of their potential use in cellular delivery. Appl Clay Sci 55, 62–69.
879 https://doi.org/10.1016/j.clay.2011.10.006

880 Quevedo, A.C., Lynch, I., Valsami-Jones, E., 2021. Silver nanoparticle induced toxicity
881 and cell death mechanisms in embryonic zebrafish cells. Nanoscale 13, 6142–
882 6161. https://doi.org/10.1039/D0NR09024G

883 Runa, S., Lakadamyali, M., Kemp, M.L., Payne, C.K., 2017. TiO_2 Nanoparticle-
884 Induced Oxidation of the Plasma Membrane: Importance of the Protein Corona. J
885 Phys Chem B 121, 8619–8625. https://doi.org/10.1021/acs.jpcb.7b04208

886 Sacchetti, C., Motamedchaboki, K., Magrini, A., Palmieri, G., Mattei, M., Bernardini,
887 S., Rosato, N., Bottini, N., Bottini, M., 2013. Surface Polyethylene Glycol
888 Conformation Influences the Protein Corona of Polyethylene Glycol-Modified
889 Single-Walled Carbon Nanotubes: Potential Implications on Biological
890 Performance. ACS Nano 7, 1974–1989. https://doi.org/10.1021/nn400409h

891 Saleh, N., Afrooz, A., Bisesi, J., Aich, N., Plazas-Tuttle, J., Sabo-Attwood, T., Saleh,
892 N.B., Afrooz, A.R.M.N., Bisesi, , Joseph H., Aich, N., Plazas-Tuttle, J., Sabo-
893 Attwood, T., 2014. Emergent Properties and Toxicological Considerations for
894 Nanohybrid Materials in Aquatic Systems. Nanomaterials 4, 372–407.
895 https://doi.org/10.3390/nano4020372

896 Sánchez, M., Guirado, R., Rincón, M.E., 2007. Multiwalled carbon nanotubes
897 embedded in sol–gel derived TiO2 matrices and their use as room temperature gas
898 sensors. Journal of Materials Science: Materials in Electronics 18, 1131–1136.
899 https://doi.org/10.1007/s10854-007-9144-5

900 Scott, J., Belden, J.B., Minghetti, M., 2021. Applications of the RTgill-W1 Cell Line for
901 Acute Whole-Effluent Toxicity Testing: In Vitro–In Vivo Correlation and
902 Optimization of Exposure Conditions. Environ Toxicol Chem 40, 1050–1061.
903 https://doi.org/10.1002/etc.4947

904 Sharma, H.K., Sharma, S.K., Vemula, K., Koirala, A.R., Yadav, H.M., Singh, B.P.,
905 2021. CNT facilitated interfacial charge transfer of TiO2 nanocomposite for
906 controlling the electron-hole recombination. Solid State Sci 112, 106492.
907 https://doi.org/10.1016/j.solidstatesciences.2020.106492

908 Shimizu, Y., Ateia, M., Wang, M., Awfa, D., Yoshimura, C., 2019. Disinfection
909 mechanism of E. coli by CNT-TiO2 composites: Photocatalytic inactivation vs.
910 physical separation. Chemosphere 235, 1041–1049.
911 https://doi.org/10.1016/j.chemosphere.2019.07.006

912 Siegrist, K.J., Reynolds, S.H., Kashon, M.L., Lowry, D.T., Dong, C., Hubbs, A.F.,
913 Young, S.-H., Salisbury, J.L., Porter, D.W., Benkovic, S.A., McCawley, M.,
914 Keane, M.J., Mastovich, J.T., Bunker, K.L., Cena, L.G., Sparrow, M.C., Sturgeon,
915 J.L., Dinu, C.Z., Sargent, L.M., 2014. Genotoxicity of multi-walled carbon
916 nanotubes at occupationally relevant doses. Part Fibre Toxicol 11, 6.
917 https://doi.org/10.1186/1743-8977-11-6

918 Sit, I., Xu, Z., Grassian, V.H., 2019. Plasma protein adsorption on TiO2 nanoparticles:
919 Impact of surface adsorption on temperature-dependent structural changes.
920 Polyhedron 171, 147–154. https://doi.org/10.1016/J.POLY.2019.06.036

921 Sun, Q., Kanehira, K., Taniguchi, A., 2016. Low doses of TiO_2 -polyethylene glycol
922 nanoparticles stimulate proliferation of hepatocyte cells. Sci Technol Adv Mater
923 17, 669–676. https://doi.org/10.1080/14686996.2016.1239499

924 Tedja, R., Lim, M., Amal, R., Marquis, C., 2012. Effects of Serum Adsorption on
925 Cellular Uptake Profile and Consequent Impact of Titanium Dioxide Nanoparticles
926 on Human Lung Cell Lines. ACS Nano 6, 4083–4093.
927 https://doi.org/10.1021/nn3004845

928 Tenzer, S., Docter, D., Kuharev, J., Musyanovych, A., Fetz, V., Hecht, R., Schlenk, F.,
929 Fischer, D., Kiouptsi, K., Reinhardt, C., Landfester, K., Schild, H., Maskos, M.,
930 Knauer, S.K., Stauber, R.H., 2013. Rapid formation of plasma protein corona
931 critically affects nanoparticle pathophysiology. Nat Nanotechnol 8, 772–781.
932 https://doi.org/10.1038/nnano.2013.181

933 Uboldi, C., Urbán, P., Gilliland, D., Bajak, E., Valsami-Jones, E., Ponti, J., Rossi, F.,
934 2016. Role of the crystalline form of titanium dioxide nanoparticles: Rutile, and
935 not anatase, induces toxic effects in Balb/3T3 mouse fibroblasts. Toxicology in
936 Vitro 31, 137–145. https://doi.org/10.1016/j.tiv.2015.11.005

Vevers, W.F., Jha, A.N., 2008. Genotoxic and cytotoxic potential of titanium dioxide (TiO2) nanoparticles on fish cells in vitro. Ecotoxicology 17, 410–420. https://doi.org/10.1007/s10646-008-0226-9

Vijayalakshmi, U., Chellappa, Anjaneyulu, Manivasagam, G., 2015. Preparation and evaluation of the cytotoxic nature of TiO2 nanoparticles by direct contact method. Int J Nanomedicine 31. https://doi.org/10.2147/IJN.S79978

Vranic, S., Gosens, I., Jacobsen, N.R., Jensen, K.A., Bokkers, B., Kermanizadeh, A., Stone, V., Baeza-Squiban, A., Cassee, F.R., Tran, L., Boland, S., 2017. Impact of serum as a dispersion agent for in vitro and in vivo toxicological assessments of TiO2 nanoparticles. Arch Toxicol 91, 353–363. https://doi.org/10.1007/s00204-016-1673-3

W. Oh, Feng-jun Zhang, Ming-liang Chen, 2009. Preparation of MWCNT/TiO2 Composites by Using MWCNTs and Titanium(IV) Alkoxide Precursors in Benzene and their Photocatalytic Effect and Bactericidal Activity. Bull Korean Chem Soc 30, 2637–2642. https://doi.org/10.5012/bkcs.2009.30.11.2637

Wang, J., Fan, Y., 2014. Lung Injury Induced by TiO2 Nanoparticles Depends on Their Structural Features: Size, Shape, Crystal Phases, and Surface Coating. Int J Mol Sci 15, 22258–22278. https://doi.org/10.3390/ijms151222258

Wang, J., Lin, Y., Pinault, M., Filoramo, A., Fabert, M., Ratier, B., Bouclé, J., Herlin-Boime, N., 2015. Single-Step Preparation of TiO $_2$ /MWCNT Nanohybrid Materials by Laser Pyrolysis and Application to Efficient Photovoltaic Energy Conversion. ACS Appl Mater Interfaces 7, 51–56. https://doi.org/10.1021/am507179c

Wang, X., Xia, T., Ntim, S.A., Ji, Z., George, S., Meng, H., Zhang, H., Castranova, V., Mitra, S., Nel, A.E., 2010. Quantitative Techniques for Assessing and Controlling the Dispersion and Biological Effects of Multiwalled Carbon Nanotubes in Mammalian Tissue Culture Cells. ACS Nano 4, 7241–7252. https://doi.org/10.1021/nn102112b

Wheeler, K.E., Chetwynd, A.J., Fahy, K.M., Hong, B.S., Tochihuitl, J.A., Foster, L.A., Lynch, I., 2021. Environmental dimensions of the protein corona. Nat Nanotechnol 16, 617–629. https://doi.org/10.1038/s41565-021-00924-1

Yoon, C.-J., Lee, S.-H., Kwon, Y.-B., Kim, K., Lee, K.-H., Kim, S.M., Kim, Y.-K., 2021. Fabrication of sustainable and multifunctional TiO2@carbon nanotube nanocomposite fibers. Appl Surf Sci 541, 148332. https://doi.org/10.1016/j.apsusc.2020.148332

Yurdakök-Dikmen, B., Vejselova, D., Kutlu, H.M., Filazi, A., Erkoç, F., 2018. Effects of synthetic pyrethroids on RTG-2 cells. Toxin Rev 37, 304–312. https://doi.org/10.1080/15569543.2017.1366922

Zhang, T., Tang, M., Yao, Y., Ma, Y., Pu, Y., 2019. <p>MWCNT interactions with protein: surface-induced changes in protein adsorption and the impact of protein

corona on cellular uptake and cytotoxicity</p>. Int J Nanomedicine Volume 14, 993–1009. https://doi.org/10.2147/IJN.S191689

Zhang, Ting, Tang, M., Kong, L., Li, H., Zhang, Tao, Zhang, S., Xue, Y., Pu, Y., 2012. Comparison of cytotoxic and inflammatory responses of pristine and functionalized multi-walled carbon nanotubes in RAW 264.7 mouse macrophages. J Hazard Mater 219–220, 203–212. https://doi.org/10.1016/j.jhazmat.2012.03.079

Zhang, Y., Wang, B., Meng, X., Sun, G., Gao, C., 2011a. Influences of Acid-Treated Multiwalled Carbon Nanotubes on Fibroblasts: Proliferation, Adhesion, Migration, and Wound Healing. Ann Biomed Eng 39, 414–426. https://doi.org/10.1007/s10439-010-0151-y

Zhang, Y., Wang, B., Meng, X., Sun, G., Gao, C., 2011b. Influences of Acid-Treated Multiwalled Carbon Nanotubes on Fibroblasts: Proliferation, Adhesion, Migration, and Wound Healing. Ann Biomed Eng 39, 414–426. https://doi.org/10.1007/s10439-010-0151-y

Zhao, X., Jia, Q., Song, N., Zhou, W., Li, Y., 2010. Adsorption of Pb(II) from an aqueous solution by titanium dioxide/carbon nanotube nanocomposites: Kinetics, thermodynamics, and isotherms. J Chem Eng Data 55, 4428–4433. https://doi.org/10.1021/je100586r

Zhou, L., Forman, H.J., Ge, Y., Lunec, J., 2017. Multi-walled carbon nanotubes: A cytotoxicity study in relation to functionalization, dose and dispersion. Toxicology in Vitro 42, 292–298. https://doi.org/10.1016/j.tiv.2017.04.027

Zouzelka, R., Kusumawati, Y., Remzova, M., Rathousky, J., Pauporté, T., 2016. Photocatalytic activity of porous multiwalled carbon nanotube-TiO2 composite layers for pollutant degradation. J Hazard Mater 317, 52–59. https://doi.org/10.1016/J.JHAZMAT.2016.05.056